



Minerva Access is the Institutional Repository of The University of Melbourne

Author/s:

Regattieri, E;Zanchetta, G;Isola, I;Zanella, E;Drysdale, RN;Hellstrom, JC;Zerboni, A;Dallai, L;Tema, E;Lanci, L;Costa, E;Magri, F

Title:

Holocene Critical Zone dynamics in an Alpine catchment inferred from a speleothem multiproxy record: disentangling climate and human influences

Date:

2019-12-01

Citation:

Regattieri, E., Zanchetta, G., Isola, I., Zanella, E., Drysdale, R. N., Hellstrom, J. C., Zerboni, A., Dallai, L., Tema, E., Lanci, L., Costa, E. & Magri, F. (2019). Holocene Critical Zone dynamics in an Alpine catchment inferred from a speleothem multiproxy record: disentangling climate and human influences. *Scientific Reports*, 9 (1), <https://doi.org/10.1038/s41598-019-53583-7>.

Persistent Link:

<https://hdl.handle.net/11343/240772>

License:

[CC BY](#)

OPEN

Holocene Critical Zone dynamics in an Alpine catchment inferred from a speleothem multiproxy record: disentangling climate and human influences

Eleonora Regattieri^{1,2*}, Giovanni Zanchetta^{1,3}, Ilaria Isola³, Elena Zanella⁴, Russell N. Drysdale^{5,6}, John C. Hellstrom⁷, Andrea Zerboni⁸, Luigi Dallai², Evdokia Tema⁴, Luca Lanci⁹, Emanuele Costa⁴ & Federico Magri¹⁰

Disentangling the effects of climate and human impact on the long-term evolution of the Earth Critical Zone is crucial to understand the array of its potential responses to the ongoing Global Change. This task requires natural archives from which local information about soil and vegetation can be linked directly to climate parameters. Here we present a high-resolution, well-dated, speleothem multiproxy record from the SW Italian Alps, spanning the last ~10,000 years of the present interglacial (Holocene). We correlate magnetic properties and the carbon stable isotope ratio to soil stability and pedogenesis, whereas the oxygen isotope composition is interpreted as primarily related to precipitation amount, modulated at different timescales by changes in precipitation source and seasonality. During the 9.7–2.8 ka period, when anthropic pressure over the catchment was scarce, intervals of enhanced soil erosion are related to climate-driven vegetation contractions and occurred during drier periods. Immediately following the onset of the Iron Age (ca. 2.8 ka), by contrast, periods of enhanced soil erosion coincided with a wetter climate. We propose that the observed changes in the soil response to climate forcing were related to early anthropogenic manipulations of Earth's surface, which made the ECZ more sensitive to climate oscillations.

The Earth's Critical Zone (ECZ) is the complex system of coupled physical, chemical, biological, and geological processes operating together to support life at the Earth's surface. This dynamic interface extends from the vegetation top to the base of active groundwater, and is a constantly evolving envelope in which the soil represents a key component¹. This zone is termed "critical" because it regulates the natural habitat and determines the availability of life-sustaining resources, but also because it is increasingly impacted upon human activities, especially land-use and land-cover change, which have long-lasting effects on the near-surface environment processes². Natural ECZ functioning is regulated largely by climate through changes in temperature and hydrology, which impinge upon vegetation, soil, topography, weathering and erosion rates². Understanding ECZ dynamics requires interdisciplinary approaches that span wide spatial and temporal scales³. Natural archives recording both soil processes and climate evolution are required to understand how soil development responds to climate variability and to human activity. Lake sediments and loess–paleosol sequences have intensively been studied in this context^{4–6}.

¹Dipartimento di Scienze della Terra, University of Pisa, Via S. Maria 53, 56126, Pisa, Italy. ²Istituto di Geoscienze e Georisorse, IGG-CNR, Via Moruzzi 1, 56126, Pisa, Italy. ³Istituto Nazionale di Geofisica e Vulcanologia INGV, Via della Faggiola 32, 56126, Pisa, Italy. ⁴Dipartimento di Scienze della Terra, University of Torino, Via Valperga Caluso 35, 10125, Torino, Italy. ⁵Department of Resource Management and Geography, University of Melbourne, Victoria, 3010, Australia. ⁶EDYTEM, UMR CNRS 5204, Université de Savoie-Mont Blanc, 73376, Le Bourget du Lac cedex, France. ⁷School of Earth Sciences, University of Melbourne, Victoria, 3010, Australia. ⁸Dipartimento di Scienze della Terra "A. Desio", University of Milan, Via Mangiagalli 34, I-20133, Milano, Italy. ⁹Dipartimento di Scienze Pure e Applicate, University of Urbino, Piazza della Repubblica 13, 61029, Urbino, Italy. ¹⁰Associazione Gruppi Speleologici Piemontesi AGSP-Club Alpino Italiano, Torino, Italy. *email: eleonora.regattieri@unipi.it

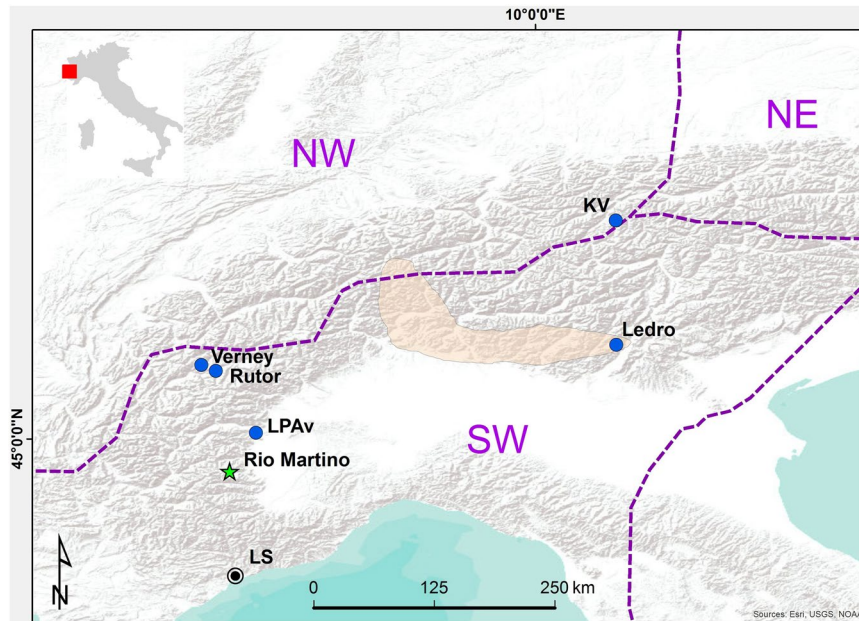


Figure 1. Location of Rio Martino Cave and of other sites mentioned in the text. Pink shadow indicates the area investigated in the synthesis on S Alps flood activity³⁰; LS-Area of the cluster of deep-seated large scale landslides⁴⁵; Ledro-Lake Ledro²⁹; KV-Kauner Valley (tree-line elevation, Fig. 4);⁵³ Rutor-Rutor mire (pollen percentage, Fig. 4)⁴¹; LPAv-Lake Piccolo di Avigliana (Urtica pollen %, Fig. 4)³⁶ Vernet-Lake Verney³⁵. Division of the Alpine region is from.

Speleothems (cave mineral deposits) are formed by meteoric water and receive inputs from bedrock, soil, vegetation and the atmosphere⁷. Geochemical properties of these deposits track environmental processes operating at the catchment scale⁸, as well as climatic changes acting at the regional scale in response to global or hemispheric climate patterns⁹. Although rarely exploited in this sense, speleothems are nevertheless well suited to reconstruct past soil dynamics and their relationship with climate, allowing us to disentangle the array of potential ECZ responses to climatic and land use changes. Here we present a high-resolution, multiproxy record (magnetic properties: natural magnetization intensity, J_r , mass magnetic susceptibility, χ , stable oxygen and carbon isotope composition: $\delta^{18}\text{O}$, $\delta^{13}\text{C}$ and growth rate) obtained from a well-dated flowstone core (RMD1) from Rio Martino Cave (Piedmont, SW Italian Alps, Fig. 1), which grew continuously over the 9.7–0.4 ka interval, thus spanning most of the present interglacial¹⁰. Magnetic properties of RMD1 were investigated at high-resolution (~ 60 yr/sample), providing a record of regional paleosecular variations (PSV) of the Earth geomagnetic field during the Holocene¹⁰. Here we explore the paleoenvironmental significance of magnetic properties by comparing them to a high-resolution (~ 16 yr) stable isotope record ($\delta^{18}\text{O}$ and $\delta^{13}\text{C}$) obtained from the same core. Magnetic minerals in speleothems are mostly related to detrital input transported by infiltrating waters¹¹. The amount and distribution of the detrital component in speleothems are strongly dependent on geological, climatic, biological (including anthropic) processes governing soil formation⁷. The concentration, composition and grain size of the magnetic mineral assemblage may thus be used to reconstruct the pedological history at the catchment scale^{11–14}. The stable isotope composition can provide information on paleo-precipitation, temperature patterns and/or soil-vegetation dynamics at the surface⁷, complementing the surficial processes recorded by the magnetic properties and linking local evolution to climate changes at the regional and extra-regional scale.

By coupling these different proxies, we attempt to reconstruct soil evolution at the catchment scale during the last ~ 10 kyr and its relation to local hydroclimate. We compare our reconstruction with the regional climatic and environmental framework, and with the record of human occupation, which is a pivotal factor in determining Holocene ECZ functioning, especially in the Alpine region⁵. The aim is to connect local processes in the soil and vegetation overlying the cave system to regional (Alpine) climatic changes and anthropogenic disturbance, to give insights on the links between the evolution of the ECZ, climate and human activities in the area during the Holocene.

Settings and material. Rio Martino Cave opens at 1530 m a.s.l. in the upper Po Valley (SW Alps, Piedmont, northern Italy, Fig. 1). The catchment area lies between 1900 and 2200 m a.s.l. and is mantled by a thick (tens of meters) sedimentary cover comprising ophiolitic gravel with an abundant silty-sandy matrix, deposited and reworked by Quaternary glacial and periglacial processes. Currently, the catchment supports an alpine grassland dominated by C3 plants. The present natural timberline elevation for the southern Alps is about 2350 m⁵, thus the present vegetation is related to anthropic modifications. The cave is crossed by a permanent stream, which responds rapidly to meteoric events due to direct infiltration where the carbonate rock is closer to the surface. However, extreme discharge variations are dampened by the major contribution of slower water circulation

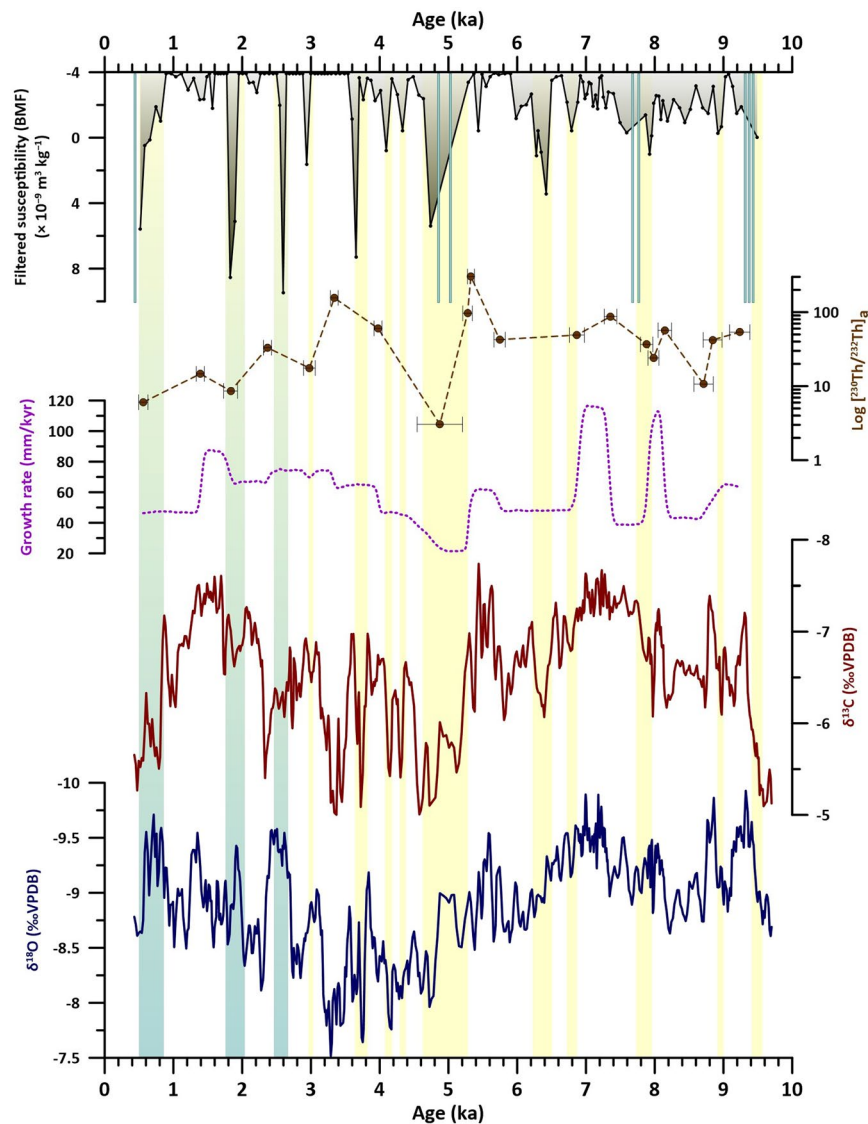


Figure 2. RMD1 proxies vs. age. From bottom: $\delta^{18}\text{O}$; $\delta^{13}\text{C}$, growth rate; $[\text{}^{230}\text{Th}/\text{}^{232}\text{Th}]_a$ for the dated points; filtered mass magnetic susceptibility (χ) series representing the background magnetic flux (BMF, see text for details), light-blue bars are the χ peaks $>12 \text{ m}^3 \text{ kg}^{-1}$ indicating the spikes of coarser material. Rectangles indicate the spikes in BMF, yellow: spikes characterized by a similar behaviour of $\delta^{13}\text{C}$ and $\delta^{18}\text{O}$; blue: intervals where $\delta^{13}\text{C}$ and $\delta^{18}\text{O}$ show an opposite pattern.

occurring within the glacial cover, which represents the main aquifer feeding the river and the cave-drip recharge system¹⁵. A detailed description of the cave and of the regional climate is provided in SOM1.

RMD1 core is 59 cm long (Fig. SOM2-1) and shows predominantly columnar calcite (SOM2). Its age-depth model is based on 20 U/Th dates and has a mean uncertainty of 0.15 kyr¹⁰ (SOM3).

The main magnetic carrier, identified through Isothermal Remanent Magnetization (IRM) acquisition curves, is low-coercivity (saturation around 0.3 T) (titano)magnetite of detrital origin¹⁰. Hysteresis loops show that the magnetic grain-size is mostly in the single-domain (SD) to pseudo-single-domain (PSD) range. Some samples (mostly associated with J_r and χ spikes) also show the occurrence of magnetite in the multi-domain (MD) range¹⁰. The IRM is of detrital origin (DRM), i.e. acquired and locked-in soon after the calcium carbonate film deposition on the speleothem surface¹¹.

Results and paleoenvironmental significance of RMD1 proxies. Assuming a constant diamagnetic contribution mostly related to the predominant calcite fraction, the relative variability of mass magnetic susceptibility (χ) represents variations in the concentration of magnetic minerals. A mean background value of $-4 \times 10^{-9} \text{ m}^3 \text{ kg}^{-1}$ can be assumed for Rio Martino speleothem, while higher values correspond to the detrital input¹⁰. This is corroborated by the high correlation ($r=0.87$) observed between χ and the natural magnetization intensity (J_r)¹⁰. The χ depth-series of RMD1 consists mostly of a prevailing diamagnetic phase with small negative values, alternating with large positive spikes of up to $970 \times 10^{-9} \text{ m}^3 \text{ kg}^{-1}$ (Fig. SOM2-1). Major spikes are

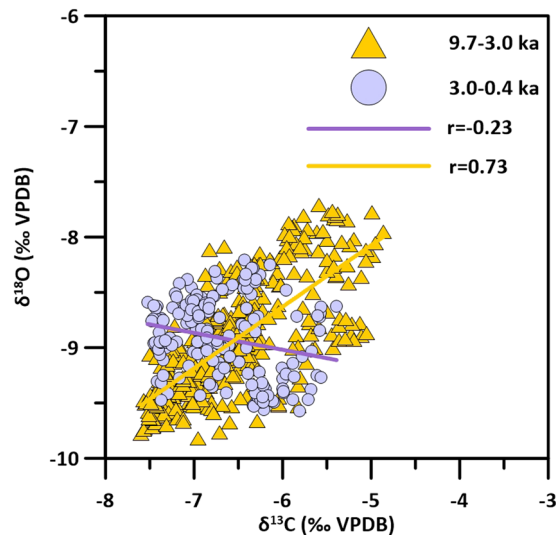


Figure 3. Correlations plot of $\delta^{13}\text{C}$ and $\delta^{18}\text{O}$ time series, previously smoothed with a 5-points running average.

associated with coarser detrital grains containing small serpentinite lithics. Coarser detrital particles were likely deposited onto the flowstone by cave stream waters (as opposed to vadose drip waters) as part of their suspended load during flood events, or immediately after in the back-flooding phase¹⁶. In Rio Martino Cave, floods are associated with fast infiltration directly through the carbonate bedrock and occur mostly during episodic intense precipitation events and/or during snow-melt peaks in spring¹⁵. Aside from the major spikes, variations in the $-4 \times 10^{-9} \text{ m}^3 \text{ kg}^{-1}$ to $\sim 12 \times 10^{-9} \text{ m}^3 \text{ kg}^{-1}$ range, representing $\sim 84\%$ of χ data, can be assumed as representative of changes in the concentration of fine-grained material deposited via diffuse infiltration through the drip-feeding network. This fine-grained material is a flux of soil and regolith particles illuviated from the surface¹⁶. Soils of the Rio Martino catchment have developed on glacially ophiolitic sediments. Pedogenic, inorganic magnetite, formed by weathering of the iron-rich parent material, is the main component of the BMF signal (SOM4). At Rio Martino, this likely stems from the contribution of the “slow” component of the aquifer, which circulates in the glacial cover sediment. Thus, it can be used to infer changes in the background flux of material derived from the overlying soil and debris cover and delivered via drip water. To better highlight this subtle variability, we filtered the χ time series by removing the spikes related to the coarser fraction (i.e. above $12 \times 10^{-9} \text{ m}^3 \text{ kg}^{-1}$) and the values lower than $-4 \times 10^{-9} \text{ m}^3 \text{ kg}^{-1}$, producing a time series of background magnetic flux (herein BMF, Fig. 2). The detrital origin of the BMF can be further tested by comparing it with the activity ratio between the radiogenic ^{230}Th and the detrital ^{232}Th (i.e. $[^{230}\text{Th}/^{232}\text{Th}]$) of the dated samples, an independent proxy for detrital contamination¹⁷. Despite the very coarse temporal resolution, the $[^{230}\text{Th}/^{232}\text{Th}]$ curve does show a similar pattern to the BMF series (Fig. 2). Changes in the detrital input can be related to changes in soil erosion rates and/or to changes in infiltration rates^{13,14,18}.

Both stable isotope time series show similar multi-millennial trends from the base up to ca. 1.5 ka. Beyond this, the two series diverge, with decreasing $\delta^{18}\text{O}$ values paired to strongly increasing $\delta^{13}\text{C}$ (Fig. 2). Superimposed on this are several multi-centennial oscillations. From the base of the record up to 2.8 ka, oscillations are mostly in phase between the two isotope series. Conversely, from 2.8 ka the two centennial patterns appear anticorrelated, and prominent intervals of negative $\delta^{18}\text{O}$ values are concomitant with $\delta^{13}\text{C}$ increases (Fig. 2). Pearson r values between the two series, previously smoothed using a five-point running average, support the visual correlation (Fig. 3): in the interval from 9.7 to 3.0 ka there is a strong, statistically significant, positive correlation ($r = 0.73$; $n = 427$), which becomes weakly negative from 3.0 ka afterwards ($r = -0.23$, $n = 164$). At mid-latitudes, speleothem $\delta^{13}\text{C}$ and growth rate are related to biological CO_2 production, which is dependent from soil and vegetation conditions in the catchment^{19,20}. Warmer and wetter periods usually enhance the production of biogenic, ^{13}C -depleted CO_2 and increases the growth rate^{19,20}. Cold/dry conditions reduce the vegetation cover and the biogenic CO_2 supply, and, in mountain settings such as Rio Martino, may enhance cryogenic processes, interrupting pedogenesis and promoting soil erosion. In these settings, an increase in the persistence of snow cover may also impact the $\delta^{13}\text{C}$ by reducing the length of the plant growing season, leading to reduced biogenic CO_2 supply. Lower/higher calcite $\delta^{13}\text{C}$ values and faster/slower growth rates are therefore usually indicative of soil development/disruptions and can be related to warmer-wetter/colder-drier conditions. Additional control on the $\delta^{13}\text{C}$ is exerted by the hydrological state of the aquifer. Partial dewatering of the drip-feeding system induces solution degassing and prior calcite precipitation, leading to higher $\delta^{13}\text{C}$ during drier periods⁷.

Paleoclimatic interpretations of speleothem $\delta^{18}\text{O}$ mostly depend on cave location and setting²¹ (SOM5). In continental Europe and the Northern Alps, a positive temperature/ $\delta^{18}\text{O}$ relationship is usually reported²², whereas in the Mediterranean region a negative relationship is commonly observed between speleothem $\delta^{18}\text{O}$ and the amount of precipitation^{23,24}. Evidence for this latter “rainfall amount effect” has been reported for the Southern Alps^{25,26}. Other drivers of alpine speleothem $\delta^{18}\text{O}$ have been linked to shifts in precipitation seasonality and/or source^{27,28} (SOM5). For RMD1, several lines of reasoning (SOM5) suggest a first-order control of the amount effect on the $\delta^{18}\text{O}$ record, although this is likely modulated at different time scales by changes in seasonality or in

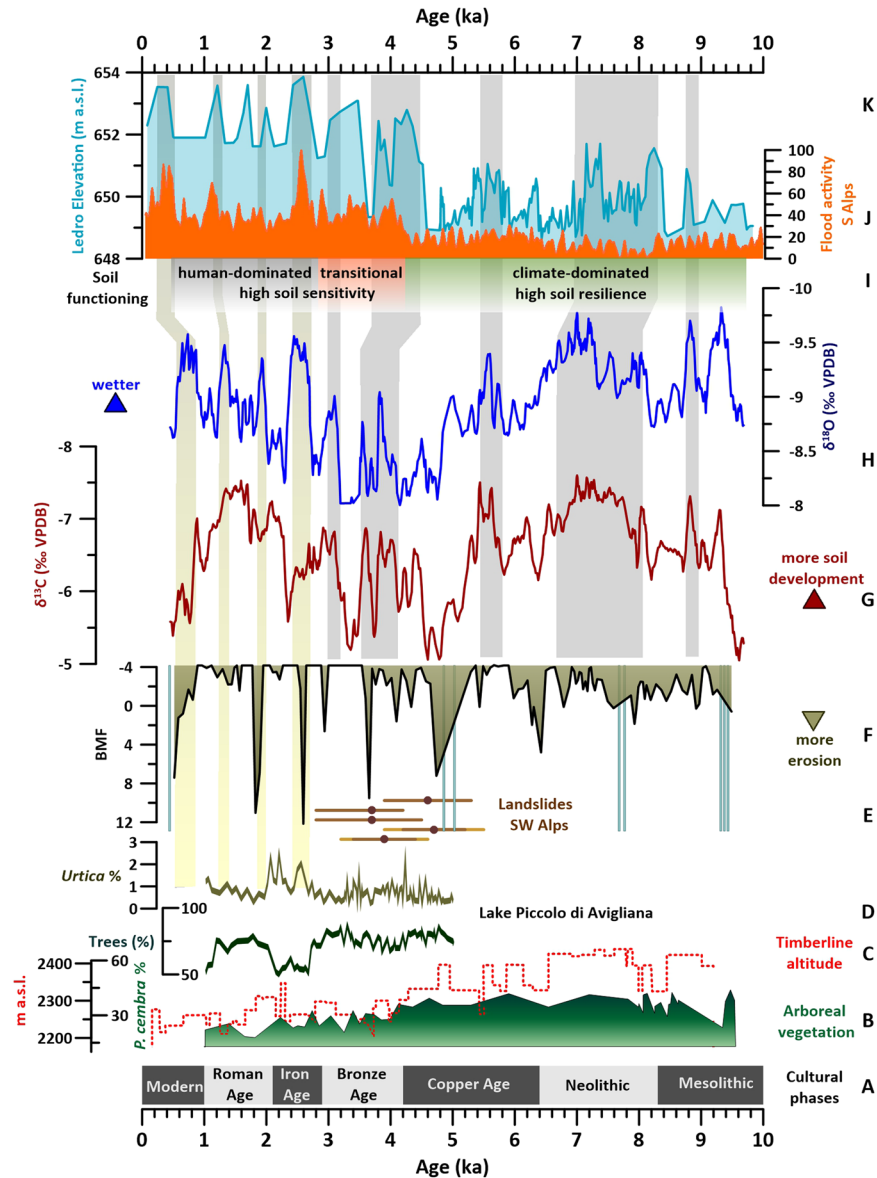


Figure 4. From bottom: A-Cultural phases in northern Italy³⁴; B-*P. cembra* pollen percentages from Rutor Mire, SWAlps⁴¹; C-Alpine tree-line altitude from Kauner Valley⁵³; D-pollen related to anthropic impact from Lago Piccolo di Avigliana³⁶; E-ages of deep-seated landslides from SWAlps⁴⁵; F-filtered magnetic susceptibility (BMF) from RMD1, light-blue bars indicate the peaks in coarser material; RMD1 δ¹³C (G) and δ¹⁸O (H), smoothed with a 5 points running average; I-Modes of soil functioning inferred from the RMD1 record J-Synthesis of flood activity from the S Alps³⁰; K-Lake Ledro level variations²⁹.

the source of precipitation. To test this hypothesis, we compared the δ¹⁸O with the record of lake-level variations from Lake Ledro²⁹ and the synthesis of flood activity from the Southern Alps³⁰ (Fig. 4). The observed similarities especially with the Lake Ledro record, confirm the proposed interpretation and suggest that the δ¹⁸O is representative of regional paleohydrology for the whole interval considered here, and thus provides a firm hydrological basis against which compare the proxies related to soil conditions (i.e. the BMF and the δ¹³C). Despite the good agreement between RMD1 δ¹⁸O and the Ledro record at the multi-centennial to millennial-scale (Fig. 4), the first part of the Holocene (i.e. up to ca. 5 ka) appears drier at Ledro whereas the RMD1 δ¹⁸O record shows relatively low values (i.e. wetter conditions). Changes in precipitation seasonality may explain the apparent discrepancy between drier conditions inferred from lake-level reconstructions and wetter conditions inferred from speleothem, because lower summer precipitation would increase the proportion of ¹⁸O-depleted winter precipitation, leading to more negative calcite δ¹⁸O values (SOM 5). A pollen-based quantitative reconstruction of winter and summer precipitation³¹ shows that extreme seasonality existed at Ledro only up to 8.5 ka, whereas the Mid- to Late Holocene was characterized by an increase in both summer and winter precipitation³¹. The most negative δ¹⁸O values observed in RMD1 occur prior to 8.5 ka and can be addressed to an additional influence of seasonality. On the contrary, the mismatching between 8.5 and 5 ka requires an alternative explanation. A pollen-based temperature reconstruction

from the same study shows higher summer temperature at Ledro during the Early to Mid-Holocene³¹. This would cause higher lake-water evaporation rates and consequent lowering of the lake level, thus better explaining discrepancies between RMD1 $\delta^{18}\text{O}$ and Lake Ledro in this interval. This is further supported by the occurrence of the lowest $\delta^{13}\text{C}$ values in the first part (up to 5 ka) of the RMD1 record, because the $\delta^{13}\text{C}$ is influenced by precipitation, but also by temperature, with warmer conditions enhancing soil biological activity¹⁹.

Near-surface dynamics at Rio Martino: disentangling climatic and human influences. The comparison among the different RMD1 proxies shows that for the whole record most of the increases in BMF correspond to increases in $\delta^{13}\text{C}$ and, in most cases, to a decrease in growth rate (Fig. 2). This is consistent with a close link between the soil status and vegetation on the one hand, and the detrital influx on the other, suggesting that the latter is dependent mostly on soil conditions. Between 9.7 and 2.8 ka, most of the increases in BMF and $\delta^{13}\text{C}$ also correspond to increases in $\delta^{18}\text{O}$, indicating drier conditions (Fig. 2). This suggests that infiltration rates are not exerting a major control on the long-term pattern of soil erosion, whose increases appear related to periods of reduced precipitation and possibly cooler conditions, reducing the vegetation cover and enhancing the surficial erosion. Clearly, occasional heavy-rain events may have favoured the downward transport of detrital material, as suggested by the magnetic spikes, but they should have less impact on the slow-flow component of the aquifer through which the BMF is delivered to the flowstone.

Between 9.7 and 9.3 ka the RMD1 record shows increasing precipitation corresponding to a decrease in the BMF (Fig. 4), both indicative of post-glacial soil stabilization. The occurrence of intense precipitation events mobilizing coarser material, likely abundant in the catchment after the glacial retreat, is apparent (Fig. 4). Between 9.3 and 6.4 ka, the record shows the highest levels of precipitation and the maximum input of soil biogenic CO_2 . Intervals of reduced precipitation and possibly temperature occur at 9.2 ka and between 8.6 and 8.2 ka. These events show a timing agreement to the widely recorded climate anomalies at 9.2 ka³² and 8.2 ka³³, but are not really prominent in the BMF record, which, within the 9.3–6.4 ka period, shows the highest background values and a muted variability (Fig. 3). The timberline for the western Alps was likely above 2350 m a.s.l. between 8.8 and 5.7 ka³⁴. The background BMF over this period likely indicates a steady flux of material illuviated from a well-developed forest soil, where an increase in organic acids from roots and the litter boosted the mobility of Fe in the upper soil horizons and its translocation downward³⁵. If we consider the anthropic influence, it is generally accepted that Mesolithic to Neolithic alpine hunter/gatherers caused only temporary ecosystem disturbances by fire intensification, rather than shaping anthropogenic landscapes^{5,34,36}. Only sparse archaeological evidence is found for Neolithic exploitation of the high-altitude Alpine belt (i.e. above 2000 m)³⁷, although alpine materials and artefacts were exchanged over great distances³⁷. In the Rio Martino area, an extensive trade network likely already existed in the late Neolithic due to the importance of nearby Mont Viso as a source of greenstone axes³⁷. However, human impact on the local ECZ dynamics should have been almost negligible (especially if compared with nearby lowlands), and the arboreal cover over the cave catchment would have limited soil erosion and the transport of detrital material, thus dampening the influence on soil of centennial-scale precipitation (and temperature) variability, as well as reducing the impact of extreme rain events.

Between 6.4 and 4.6 ka, the RMD1 record shows a trend of decreasing precipitation, reduced soil activity, and several multi-centennial increases in detrital influx. A prominent deterioration is apparent in all proxies between 6.4 and 6.0 ka (Fig. 4). Although not well expressed in the Lake Ledro record, it matches a dry/cold interval detected in several other Mediterranean terrestrial and marine records^{38,39}. Also, between 5.2 and 4.6 ka, RMD1 shows another interval of higher soil erosion, corresponding to prominent drier conditions (Fig. 4). The pronounced lowering of growth rate (Fig. 3) suggests a temperature decrease. The maximum of this interval is also characterized by spikes in the coarser fraction, indicating an increase of floods and/or in the supply of erodible detrital material in the catchment, potentially related to a reduced arboreal cover. At the regional scale, the regime of soil formation from ~5.2 ka appears to change towards more unstable conditions and higher erosion rates⁵, whereas forest decline and lowering of the timberline, triggered by repeated phases of climate instability, are increasingly evident from 5.6 ka onwards^{40,41}. In the Alps, the 6.4–4.6 ka interval also corresponds to the Early to Late Copper Age³⁴. Sporadic occupation of high-altitude Alpine sites since this period is reported from archaeological remains and charcoal accumulation in lake sediments^{5,40}. It has been suggested that climatic instability during the Mid-Holocene may have been a precursor to the development of high-altitude pastoralism rather than an obstacle for such activity due to increased pressures on lowland pasture and opened-up higher altitude pastures as tree-lines retreated³⁷. However, persistent human impact on vegetation during the Copper Age was either absent or undetectable in mid- to high-altitude palynological records from both the northern and the Southern Alps^{36,42}. Accordingly, at Rio Martino intervals of soil erosion appear to occur during drier conditions, and can be related to climate-driven vegetation contractions. From 4.6 ka, precipitation and soil conditions recovered at Rio Martino, but both remained highly variable at the multi-centennial scale until ~3.0 ka (Fig. 4), with abrupt and repeated drier intervals associated with a decrease in soil activity and increased detrital influx. At the regional scale, the period between ca. 5.5 and 3.0 ka corresponds to a substantial rearrangement of forest composition and further reduction in arboreal cover^{34,41}, a widespread expansion of small alpine glaciers (the so-called Alpine Neoglacial period^{43,44}), and an increased frequency of large-scale landslides in the SW Alps and the Apennines, which was related to periods of heavy rainfall^{45,46} (Fig. 4). Over this time interval, there is much evidence for the onset of pervasive and diffuse anthropogenic, zoo-geomorphological disturbances (*sensu*^{47,48}), with most records indicating that humans became a major geomorphological agent in shaping high-altitude Alpine environments after the Copper/Bronze Age transition (~4.2 ka, Fig. 4)^{5,6,34,37,49}. In the surrounding Alpine foothills, increasing long-term trends in anthropogenic pollen reflect a more intensive human-impacted environment, because of a major change in agricultural practices related to the adoption of Bronze tools^{36,42}. Contemporaneous dramatic changes in the engagement with the high-altitude Alpine zone are suggested by the appearance of stone-built structures in the SW Alps between ca. 4 and 3 ka³⁷, which is consistent with the development of persistent

summer settlements. Interestingly, from 3.9 ka onward, BMF/ $\delta^{13}\text{C}$ spikes become more abrupt and shorter, and there is an overall lowering of the BMF background (Fig. 4). The onset of a human-induced “metapedogenetic phase”, characterized by definitive deforestation and erosion of the upper organic horizon and was identified between 4.3 and 2.6 ka in the record of Lake Verney from the French-Italian Alps³⁵, located at 2188 m a.s.l, thus at an altitude comparable with Rio Martino. This is consistent with the higher sensitivity of soil conditions to hydrological variations apparent from our record since ca. 4.4–4.2 ka (Fig. 4), related to deforestation and increasing anthropic pressure over the catchment.

From 2.8 ka onward, the RMD1 carbon and oxygen time series largely decouple (Fig. 3). Intervals of depressed soil biological activity (higher $\delta^{13}\text{C}$) and enhanced detrital flux (higher BMF) appear to coincide with prominent intervals of lower $\delta^{18}\text{O}$, indicating wetter conditions. Negative peaks in the $\delta^{18}\text{O}$ curve still resemble lake-level variations at Ledro (Fig. 4), and its general trend mimics the regional precipitation increase observed since 4.4 ka^{5,29,50}. Thus, hydrology was still the first-order driver of $\delta^{18}\text{O}$, whereas there is a change in the $\delta^{13}\text{C}$ response to hydrological variations. Following this, prominent intervals of abrupt increases in precipitation between 2.8 and 2.3 ka, at ca. 2.0 ka and between 1.0 and 0.5 ka are marked by deterioration of soil conditions, and higher erosion (Fig. 4). The pattern of variations in the different RMD1 proxies suggests a change in the soil response to climate forcing, and unprecedented environmental modifications initiated at ca. 2.8 ka. Noteworthy, this change corresponds to the beginning of the Iron Age in northern Italy³⁴. At the Bronze to Iron Age transition (2.9–2.8 ka), increasing minerogenic input from soil overlaps with the widespread occurrence of anthropic indicators, such as *Urtica* in several lacustrine pollen records from both the northern and southern Alpine foothills⁴², and notably in the pollen record from Lake Piccolo di Avigliana³⁶, not far from Rio Martino (Figs. 1 and 4). Progressively stronger impacts was related to pronounced demographic expansion, with reinforcement of herding at high-altitude sites paired with the spread of metal tools for agriculture and forest exploitation (Fig. 4)^{5,34,40,49}. Interestingly, in the southern Alps the commencement of dairy production, especially that of hard cheese, is dated by some authors to the Late Bronze/Early Iron Age⁵¹. Milk cannot be stored for long periods and deteriorates rapidly, whereas cheese can be easily stored and transported. The development of dairy techniques allowed the use of upland summer pasture and the exploitation of the high-quality Alpine pastures for grazing, triggering the onset of seasonal transhumance and the rise of the modern-time “Alpine economy”⁵¹. This widespread land-use change, paired with climate-related regression of the timberline, would have had a dramatic impact on soil conditions. Therefore, we correlate changes in the relative pattern of hydrological variations and soil conditions at Rio Martino since 2.8 ka, -i.e. enhanced erosion occurring during wetter rather than drier periods- to the establishment of intensive grazing due to the definitive settlement of high-altitude pastoralism in the catchment. This triggered a rapid degradation and erosion of soil horizons, leading to an overall increase in the vulnerability of soils to climate change. In particular, it seems to have led to a marked enhancement of surface erosion and soil loss during periods when infiltration rates were high, likely resulting in a permanent shift from arboreal to the present-day shrub-and-grasslands vegetation.

In summary, the combined variability of magnetic parameters and the stable oxygen and carbon isotope composition from a Rio Martino speleothem provides new insights into the links between climate, soil stability and evolution, and land-use changes for the area during the Holocene, and has far-reaching implications for our understanding of the interplay between climate, human activities and ECZ dynamics. From 9.8 ka to 4.2 ka, when anthropic pressure at high-altitude Alpine sites was low^{34–36}, intervals of soil instability and increasing erosion occurred during drier and possibly cooler periods, and were linked to climate-driven reductions in vegetation cover that are traceable at the regional scale. This influenced soil erosion and enhanced the detrital influx. Wetter and warmer periods, instead, promoted soil stability, with the denser vegetation retaining micrometer-scale pedogenic minerals and reducing detrital flux to the cave. Between 4.2 and 2.8 ka, intervals of high erosion were shorter, more frequent and abrupt, but still coinciding with drier periods, suggesting that soil sensitivity was enhanced by deforestation during the Bronze Age. From 2.8 ka onwards, with the beginning of the Iron Age, the onset of seasonal transhumance and the establishment of the modern “Alpine economy”⁵¹, increased exploitation of high-altitude sites resulted in a drastic change in the response of soil stability to climate variations, with intervals of soil erosion promoted by increasing precipitation. This suggests that early land-use changes made the mountain pedosphere more sensitive to climatic oscillations, and that pre-industrial human impacts profoundly modified the natural functioning of the ECZ in this Alpine catchment, causing heterogeneities in its responses to climate forcing. Our findings fit well within the recent global synthesis of land-use for the last 10 ka which reveals a planet Earth well and truly transformed by growing communities of hunter-gatherers, farmers, and pastoralists by 3 ka⁵². The RMD1 record also demonstrates that speleothem paleomagnetic properties are an effective tool to reconstruct past soil dynamics and their link with natural and anthropic processes, potentially advancing our ability to understand the present and future evolution of the ECZ and its potential responses to ongoing climate and land-uses changes.

Methods

Details of the U/Th dating, age modelling and paleomagnetic analyses have been reported previously¹⁰, and are summarized in SOM3. Samples for stable isotope analysis were drilled on a polished half of the core at 1 mm increments using a milling lathe (CNC Protosystem) at the National Institute of Geophysics and Volcanology (Pisa). Stable oxygen ($\delta^{18}\text{O}$) and carbon ($\delta^{13}\text{C}$) isotope analyses on 495 subsamples were performed with a Gas Bench II (Thermo Scientific) coupled to a Delta XP (Finnigan MAT) IRMS at the Institute of Geosciences and Earth Resources of the Italian National Research Council (IGG-CNR, Pisa). About 0.12 mg of calcite were digested in H_3PO_4 (105%) and left to react at 70 °C for 1 h. Sample results were corrected using the IAEA standard NBS-18 and a set of three internal standards, which were calibrated by inter-laboratory comparisons and using the IAEA standards NBS-18 and NBS-19 and. Results are referred to the V-PDB international standard. Analytical uncertainties are of 0.15‰ and 0.10‰ and for $\delta^{18}\text{O}$ and $\delta^{13}\text{C}$ respectively.

Received: 26 June 2019; Accepted: 2 November 2019;

Published online: 28 November 2019

References

1. Brantley, S. L., Goldhaber, M. B. & Ragnarsdottir, K. V. Crossing disciplines and scales to understand the critical zone. *Elements* **3**(5), 307–314 (2007).
2. Richter, D. B. & Mobley, M. L. Monitoring Earth's Critical Zone. *Science* **326**(5956), 1067–1068 (2009).
3. Anderson, S. P., Bales, R. C. & Duffy, C. J. Critical Zone Observatories: Building a network to advance interdisciplinary study of Earth surface processes. *Min. Mag.* **72**(1), 7–10 (2008).
4. Mannella, G. *et al.* Palaeoenvironmental and palaeohydrological variability of mountain areas in the central Mediterranean region: A 190 ka-long chronicle from the independently dated Fucino palaeolake record (central Italy). *Quat. Sci. Rev.* **210**, 190–210 (2019).
5. Arnaud, F. *et al.* Erosion under climate and human pressures: An alpine lake sediment perspective. *Quat. Sci. Rev.* **152**, 1–18 (2016).
6. Cremaschi, M. *et al.* Age, soil-forming processes, and archaeology of the loess deposits at the Apennine margin of the Po Plain (northern Italy). New insights from the Ghiardo area. *Quat. Int.* **376**, 173–188 (2015).
7. Fairchild, I. J. & Baker, A. *Speleothem science: from process to past environments* (Vol. 3). John Wiley & Sons (2012).
8. Borsato, A., Frisia, S., Fairchild, I. J., Somogyi, A. & Susini, J. Trace element distribution in annual stalagmite laminae mapped by micrometer-resolution X-ray fluorescence: implications for incorporation of environmentally significant species. *Geochim. Cosmochim. Acta* **71**(6), 1494–1512 (2007).
9. Tzedakis, P. C. *et al.* G. Enhanced climate instability in the North Atlantic and southern Europe during the Last Interglacial. *Nat. Commun.* **9**(1), 4235 (2018).
10. Zanella, E. *et al.* A 10,000 yr record of high-resolution Paleosecular Variation from a flowstone of Rio Martino Cave, Northwestern Alps, Italy. *Earth Planet. Sc. Lett.* **485**, 32–42 (2018).
11. Lascu, I. & Feinberg, J. M. Speleothem magnetism. *Quat. Sci. Rev.* **30**(23–24), 3306–3320 (2011).
12. Zhu, Z. *et al.* H. Holocene ENSO-related cyclic storms recorded by magnetic minerals in speleothems of central China. *Proc. Nat. Acad. Sci. USA* **114**(5), 852–857 (2017).
13. Jaqueto, P. *et al.* Linking speleothem and soil magnetism in the Pau d'Alho cave (central South America). *J. Geophys. Res.-Solid Earth* **121**(10), 7024–7039 (2016).
14. Bourne, M. D. *et al.* Long-term changes in precipitation recorded by magnetic minerals in speleothems. *Geology* **43**(7), 595–598 (2015).
15. Magri, Federico and Associazione Gruppi Speleologici Piemontesi (AGSP). La Grotta di Rio Martino (Valle Po-Piemonte). Eds Federico Magri. Pubs. Regione Piemonte, 5–98 (2007).
16. Bosch, R. F. & White, W. B. Lithofacies and transport of clastic sediments in karstic aquifers. In *Studies of cave sediments* Springer, Boston, MA, 1–22 (2004).
17. Hellstrom, J. U. –T. dating of speleothems with high initial ^{230}Th using stratigraphical constraint. *Quat. Geochron.* **1**(4), 289–295 (2006).
18. Regattieri, E. *et al.* Environmental variability between the penultimate deglaciation and the mid Eemian: Insights from Tana che Urla (central Italy) speleothem trace element record. *Quat. Sci. Rev.* **152**, 80–92 (2016).
19. Genty, D. *et al.* Dead carbon in stalagmites: carbonate bedrock paleodissolution vs. ageing of soil organic matter. Implications for ^{13}C variations in speleothems. *Geochim. Cosmochim. Acta* **65**(20), 3443–3457 (2001a).
20. Genty, D., Baker, A. & Vokál, B. Intra- and inter-annual growth rate of modern stalagmites. *Chem. Geol.* **176**(1–4), 191–212 (2001b).
21. Lachniet, M. S. Climatic and environmental controls on speleothem oxygen-isotope values. *Quat. Sci. Rev.* **28**, 412–432 (2009).
22. Spötl, C. & Mangini, A. Stalagmite from the Austrian Alps reveals Dansgaard–Oeschger events during isotope stage 3: Implications for the absolute chronology of Greenland ice cores. *Earth Planet. Sc. Lett.* **203**(1), 507–518 (2002).
23. Bard, E. *et al.* Hydrological conditions over the western Mediterranean basin during the deposition of the cold Sapropel 6 (ca. 175 kyr BP). *Earth Planet. Sc. Lett.* **202**, 481–494 (2002).
24. Regattieri, E. *et al.* A MIS 9/MIS 8 speleothem record of hydrological variability from Macedonia (FYROM). *Glob. Pla. Change* **162**, 39–52 (2018).
25. Columbu, A., Sauro, F., Lundberg, J., Drysdale, R. & De Waele, J. Palaeoenvironmental changes recorded by speleothems of the southern Alps (Piani Eterni, Belluno, Italy) during four interglacial to glacial climate transitions. *Quat. Sci. Rev.* **197**, 319–335 (2018).
26. Belli *et al.* Regional climate variability and ecosystem responses to the last deglaciation in the northern hemisphere from stable isotope data and calcite fabrics in two northern Adriatic stalagmites. *Quat. Sci. Rev.* **72**, 146–158 (2013).
27. Mangini, A., Spötl, C. & Verdes, P. Reconstruction of temperature in the Central Alps during the past 2000 yr from a $\delta^{18}\text{O}$ stalagmite record. *Earth Planet. Sc. Lett.* **235**(3–4), 741–751 (2005).
28. Luetscher, M. *et al.* North Atlantic storm track changes during the Last Glacial Maximum recorded by Alpine speleothems. *Nat. Commun.* **6**, 6344 (2015).
29. Magny, M. *et al.* Holocene palaeohydrological changes in the northern Mediterranean borderlands as reflected by the lake-level record of Lake Ledro, northeastern Italy. *Quat. Res.* **77**(3), 382–396 (2012).
30. Wirth, S. B., Glur, L., Gilli, A. & Anselmetti, F. S. Holocene flood frequency across the Central Alps–solar forcing and evidence for variations in North Atlantic atmospheric circulation. *Quat. Sci. Rev.* **80**, 112–128 (2013).
31. Peyron, O. *et al.* Contrasting patterns of climatic changes during the Holocene across the Italian Peninsula reconstructed from pollen data. *Clim. Past.* **9**, 1233–1252 (2013).
32. Fleitmann, D. *et al.* Evidence for a widespread climatic anomaly at around 9.2 ka before present. *Paleoceanography*, **23**(1) (2008).
33. Alley, R. B. *et al.* Holocene climatic instability: A prominent, widespread event 8200 yr ago. *Geology* **25**(6), 483–486 (1997).
34. Pini, R. *et al.* From pristine forests to high-altitude pastures: an ecological approach to prehistoric human impact on vegetation and landscapes in the western Italian Alps. *J. Ecol.* **105**(6), 1580–1597 (2017).
35. Bajard, M. *et al.* Long-term changes in alpine pedogenetic processes: Effect of millennial agro-pastoralism activities (French-Italian Alps). *Geoderma* **306**, 217–236 (2017).
36. Finsinger, W. & Tinner, W. Holocene vegetation and land-use changes in response to climatic changes in the forelands of the southwestern Alps, Italy. *J. Quat. Sci.* **21**(3), 243–258 (2006).
37. Walsh, K. & Mocchi, F. Mobility in the mountains: Late third and second millennia alpine societies' engagements with the high-altitude zones in the Southern French Alps. *Eu. J. of Archae.* **14**(1–2), 88–115 (2011).
38. Jalali, B., Sicre, M. A., Bassetti, M. A. & Kallel, N. Holocene climate variability in the north-western Mediterranean Sea (gulf of lions). *Clim. Past.* **12**, 91–120 (2016).
39. Smith, A. C. *et al.* North Atlantic forcing of moisture delivery to Europe throughout the Holocene. *Sci. Rep.* **6**, 24745 (2016).
40. Pini, R. *et al.* F. Ecological changes and human interaction in Valcamonica, the rock art valley, since the last deglaciation. *AMQ* **29**(1), 19–34 (2016).
41. Badino, F. *et al.* 8800 years of high-altitude vegetation and climate history at the Rutor Glacier forefield, Italian Alps. Evidence of middle Holocene timberline rise and glacier contraction. *Quat. Sci. Rev.* **185**, 41–68 (2018).
42. Tinner, W. *et al.* Climatic change and contemporaneous land-use phases north and south of the Alps 2300 BC to 800 AD. *Quat. Sci. Rev.* **22**(14), 1447–1460 (2003).

43. Giraudi, C. Late Holocene glacial and periglacial evolution in the upper Orco Valley, northwestern Italian Alps. *Quat. Res* **71**(1), 1–8 (2009).
44. Federici, P. R. *et al.* M. Glacial history of the Maritime Alps from the last glacial maximum to the little ice age. *Geological Society, London, Special Publications* **433**(1), 137–159 (2017).
45. Zerathe, S. *et al.* Mid-Holocene cluster of large-scale landslides revealed in the Southwestern Alps by 36Cl dating. Insight on an Alpine-scale landslide activity. *Quat. Sci. Rev.* **90**, 106–127 (2014).
46. Bertolini, G. Radiocarbon dating on landslides in the Northern Apennines (Italy). In: McInnes, Jakeways, Fairbank, Mathie, (Eds), *Landslides and Climate*. Taylor & Francis Group, London. (2007).
47. Butler, D. R. Zoogeomorphology in the Anthropocene. *Geomorphology* **303**, 146–154 (2018).
48. Zerboni, A. & Nicoll, K. Enhanced zoogeomorphological processes in arid North Africa on the human-impacted landscape of the Anthropocene. *Geomorphology* **331**, 22–35 (2019).
49. Giguet-Covex, C. *et al.* Frequency and intensity of high-altitude floods over the last 3.5 ka in northwestern French Alps (Lake Anterne). *Quat. Res.* **77**(1), 12–22 (2012).
50. Furlanetto, G. *et al.* Holocene vegetation history and quantitative climate reconstructions in a high-elevation oceanic district of the Italian Alps. Evidence for a middle to late Holocene precipitation increase. *Quat. Sci. Rev.* **200**, 212–236 (2018).
51. Pearce, M. Hard cheese: upland pastoralism in the Italian Bronze and Iron Ages. *Summer Farms: Seasonal exploitation of the uplands from prehistory to the present*. Sheffield Archaeological Monograph 16. J.R. Collins Publications 47–56 (2016)
52. Stephens, L. *et al.* Archaeological assessment reveals Earth's early transformation through land use. *Science* **365**(6456), 897–902 (2019).
53. Nicolussi, K. *et al.* Holocene tree-line variability in the Kauner Valley, Central Eastern Alps, indicated by dendrochronological analysis of living trees and subfossil logs. *Veg. Hist. Archaeobot.* **14**(3), 221–234 (2005).

Acknowledgements

We thank the Associazione Gruppi Speleologici Piemontesi (AGSP) for support during field operation. This study is founded by the University of Pisa (Fondi di Ateneo assigned to ER and GZ) and by the Australian Research Council Discovery Project scheme (grant number DP160102969, assigned to RND, JH, GZ and ER). ER also acknowledges funding from the National Geographic Society (CP-073ER-17).

Author contributions

F.M. gives support during the field work and provide data about the cave hydrological settings. E.R. and L.D. made the isotope measurements. I.I. made the sub-sampling for isotopes analyses and dating and provides Figure 1. J.C.H. provide the chronological data. E.Z., E.T., L.L., E.C. provided paleomagnetic data. A.Z. provide information regarding the anthropic background in the area. All authors discussed and interpreted the data. E.R., G.Z. and R.D. wrote the manuscript. All authors commented on early versions of the manuscript and reviewed the final version.

Competing interests

The authors declare no competing interests.

Additional information

Supplementary information is available for this paper at <https://doi.org/10.1038/s41598-019-53583-7>.

Correspondence and requests for materials should be addressed to E.R.

Reprints and permissions information is available at www.nature.com/reprints.

Publisher's note Springer Nature remains neutral with regard to jurisdictional claims in published maps and institutional affiliations.



Open Access This article is licensed under a Creative Commons Attribution 4.0 International License, which permits use, sharing, adaptation, distribution and reproduction in any medium or format, as long as you give appropriate credit to the original author(s) and the source, provide a link to the Creative Commons license, and indicate if changes were made. The images or other third party material in this article are included in the article's Creative Commons license, unless indicated otherwise in a credit line to the material. If material is not included in the article's Creative Commons license and your intended use is not permitted by statutory regulation or exceeds the permitted use, you will need to obtain permission directly from the copyright holder. To view a copy of this license, visit <http://creativecommons.org/licenses/by/4.0/>.

© The Author(s) 2019